

REGENERATIVE BRAKING AND SENSOR LESS CONTROL INTEGRATION OF RENEWABLE ENERGY RESOURCES FOR EV APPLICATIONS

1. DARNASI CHARITHA RATAN M.TECH (POWER SYSTEMS AND AUTOMATION)

2. P.MURARI HEAD OF THE DEPARTMENT

DEPARTMENT OF ELECTRICAL AND ELETRONICS ENGINEERING

SANKETIKA VIDYA PARISHAD ENGINEERING COLLEGE, VISAKHAPATNAM

ABSTRACT: -

This article offers a state-of-the-art *powertrain and controller design for an e-rickshaw* powered by RES. Brushless dc (BLDC) motor drives without Hall-effect position sensors often have delayed commutation at low and high speeds. Because of the tiny back EMF magnitude, conventional control is useless. In this example, the motor is driven across the complete range using the proposed sensor less control with commutation error compensation. A simple commutation error compensation method is developed to identify the freewheeling pulses, eliminating the need for low pass filters, and reducing control complexity for low-cost EV applications. It is also advised to use a zero-crossing detection (ZCD) approach, which eliminates the need for a separate phase compensator by automatically correcting the delay. A fixed delay digital filter removes any unwanted spikes from the ZCD circuit. Effective MPPT control is achieved by using a modified Landsman converter, which eliminates the requirement for a ripple filter at the front end and provides ripple-free current at the output. The BLDC

motor drive's capacity to regenerate energy reduces EV energy concern since thanks to the Renewable, an EV never runs out of electricity. The controller is a fuzzy logic controller based on a PI. MATLAB/Simulink Results Illustrate the System's Effectiveness.

INTRODUCTION:

The most popular electric vehicle (EV) in India is the electric rickshaw, which is an essential part of the country's public transportation infrastructure. A major concern is the battery capacity, which limits the vehicle's working range. the availability of regenerative braking, which recovers the kinetic energy of the car. The vehicle's energy is redirected back to the source, and when the battery's state of charge (SoC) rises, it becomes possible to increase battery capacity rather than increase the size of the battery, which would add to the system's weight and cost. Brushless dc (BLDC) motor drives have attracted a lot of attention in the EV market due to its high energy density and straightforward control architecture. Three mechanical sensors that are mounted on the BLDC motor's stator and are used to

operate the motor. It takes six different processing circuits to create one rotor position signal. The fragility and susceptibility to damage of these Hall-effect sensors under challenging working conditions raises questions about their reliability for EV drives. The PI controller and switching signals that produce PWM are utilised to regulate the speed of the BLDC. To achieve improved speed control and resilience, the PID controller is employed for a variety of load conditions. In high-speed range drive system applications, the commutation error in these brushless motors is found to be a very concerning problem that is causing a decline in the overall performance of the system. Commutation error is hard to eradicate since a lot of non-ideal factors negatively affect how accurate commutations are. This issue is addressed by the sensor-less control, which also enhances the drive system's aesthetic appeal. It is based on the third-harmonic compensation method. By using the virtual third harmonic to remove the commutation error, the system's performance is enhanced. The output of the motor-fed system should be constant in a range of operating conditions. This is accomplished by use of the motor-connected drive arrangement converter system. Power conversion is handled at the source by power electronics converters. Power converters are made up of power semiconductor components that can be used in both high- and low-power applications. Power converters are used to increase the energy delivered from the source. Examples of power converters include dc-dc, ac-dc, and ac-ac versions. Ordinary boost and buck-boost converters are used to raise the DC bus voltage because they are inexpensive and simple to use in a structure where the load is connected to the converter

system. However, it does not generate enough voltage gain for a high step-up application. The power converters have a large capacitor, a high percentage of passive components, and reduced efficiency. Because the landsman converter eliminates the issues and requires less components to operate than converters like SEPIC, ZETA, and Cuk, it is superior to them. To obtain a power switch, a control system must regulate it. high voltage increases from the input voltage. Traditional systems are controlled and regulated using PWM, PI, and PID control, which also provides gate signals for the power switches with the appropriate duty cycle. Fuzzy-PID control is utilised to stabilise the system so that the landsman converter may raise the DC link voltage, reduce the settling time, and provide a steady input supply for the Three Level voltage source converter (VSC). IFOC control and a BLDC motor based on back EMF estimate are combined in the fundamental implementation of the fuzzy-PID approach. The MPPT with Inc & con algorithm power maximisation method is recommended for a landsman converter (LC) supplied brushless BLDC motor to collect power from a PV system. The DC link voltage enhancement and reduced settling time of the proposed system are compared to those of the existing system.

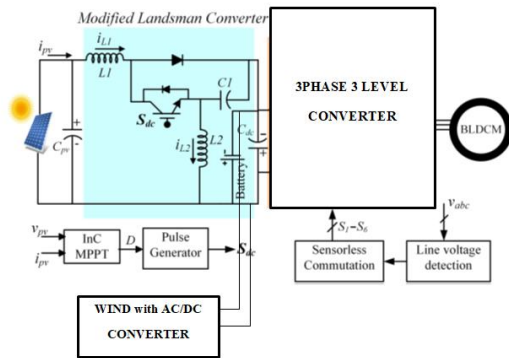


Fig 1 Block Diagram of Proposed Converter

II. PROPOSED SYSTEM

In the proposed system, as shown in figure 1, a brushless DC drive receives direct current from a PV source. This study includes a three-level VSI, a landsman converter, a single-diode PV array, wind with AC/DC, and a BLDC motor. The LC controls the high voltage gain and sends it to the VSI connected to the BLDC. By using LC, the fuzzy-PID control method seeks to achieve high voltage. This concept achieves high voltage gain and LC output voltage settling time by using the Fuzzy-PID control technique. The BLDC motor's speed and ripple reduction are managed via the Sensor less Control Technique.

III. MODELLING OF PV SYSTEM

A group of PV modules are implemented by the photovoltaic (PV) array block. The modules in each string of the array are connected in parallel and are composed of modules connected in series. The PV Array block uses a five-parameter model that contains a current source (I_L , or light-generated current), diode (I_0 and nI parameters), series resistance R_s , and shunt resistance R_{sh} to reflect the

irradiance- and temperature-dependent I-V characteristics of the modules.

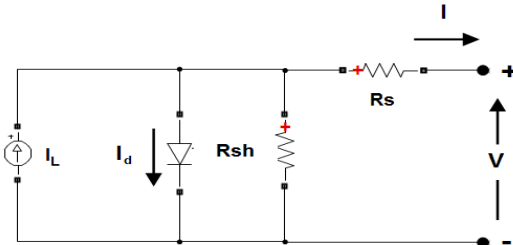


Fig2 Single Diagram of PV System

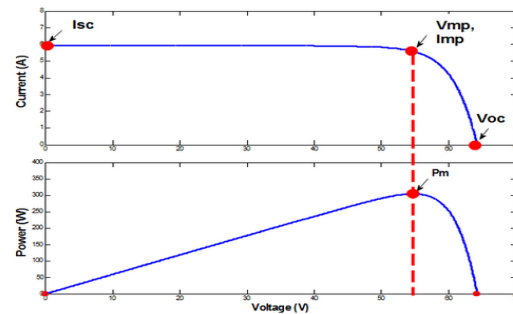


Fig3 PV characteristics

The diode I-V characteristics for a single module are specified by the formulae.

$$I_d = I_0 \left[\exp\left(\frac{V_d}{V_T}\right) - 1 \right]$$

$$V_T = \frac{kT}{q} \times nI \times N_{cell} \quad (1)$$

Diode current is represented by I_d , diode voltage by V_d , diode saturation current by I_0 , diode ideality factor by nI , Boltzmann constant by k , electron charge by q , temperature of the cell T , and number of cells N_{cell} . Indicates Quantity of Cells A 380 W peak power capacity, high-efficiency solar panel powers the electric vehicle system when connected in series. The parameters of the solar PV array and the converter are designed using the open-circuit voltage and short-circuit current. A total open-circuit voltage of 70 V

and a short-circuit current of 9.36 A are selected. Therefore, a voltage of $V_{mp} = 700.67 \text{ V}$ 47 V occurred across the solar panel when the converter attempted to operate in MPPT mode. That is comparable to $I_{mp} = I_e$.

The current flowing from the solar panel would be 380/47A8A. The MPPT algorithm is implemented using incremental conductance logic, and the maximum power point is reached when the incremental conductance (i_{pv}/v_{pv}) equals the real conductance (i_{pv}/v_{pv}). The duty ratio of the modified Landsman converter is preserved by the MPPT algorithm's configuration. The high-frequency pulse generator provides the required gate pulses to the converter. Planning here takes into consideration the ideal solar insolation. The buck-boost property of the enhanced Landsman converter manages the partial shade situation. Ideally, a 10% loss from partial shadowing may be prevented.

IV DESIGNING OF LANDSMAN CONVERTER

Increased photovoltaic (PV) power is the goal of the LC, a dc-dc converter whose performance in the CCM is reliant on the level of irradiance variation. Brushless DC motors receive improved voltage and a shorter settling time from the suggested LC. For a better, safer, and quieter BLDC motor operating, the recommended LC optimises the PV array output voltage. The DC bus voltage of the proposed BLDC system is regulated and achieves higher voltage gain because of the LC converter's operation. A switch (sdc), a capacitor (c1), and two inductors (L1, L2) make up an LC converter. The solar output is connected to the LC converter's input, and the DC capacitor (Cdc) is connected to the converter's output.

The voltage and current ratings of the solar panel are set to $i_{pv} = 8.11 \text{ A}$ and $v_{pv} = V_{mp} = 47 \text{ V}$, respectively. The input inductor of the modified Landsman converter carries the same amount of current as the rated PV panel since $i_{pv} = i_{L1} = 8.11 \text{ A}$. The following duty ratio for the dc-dc converter is anticipated:

$$D = \frac{V_{dc}}{V_{dc} + V_{pv}} = \frac{48}{48 + 46.8} = 0.506 \quad (2)$$

where V_{dc} and v_{pv} stand for the DC bus and PV panel output voltages, respectively. To find the current passing through the dc link capacitor at its maximum power, apply the following formula.

$$I_{dc} = \frac{P_{mp}}{V_{dc}} = \frac{380}{48} = 7.91 \text{ A} \quad (3)$$

PWM pulses for the converter are produced at a frequency of 20 kHz. The terms I_{L1} and I_{L2} represent the inductor currents. The output voltage ripple is constrained by the large value of the dc bus capacitor, even if a little amount of ripple is permitted to flow in the circuit to determine component size. The dc bus capacitor is enhanced by utilising the highest and lowest angular frequencies of the VSI. The LC Converter's Parameter Design is Shown in Table I.

V. PID FUZZY CONTROLLER

Fuzzy logic employed spoken expressions to represent operational laws rather than mathematical formulas. In many systems, traditional methodologies become unfeasible due to their complexity, which prevents them from being accurately represented even with complex mathematical formulae.

Parameter	Expression	Design data	Value
C_f	$\frac{D \times I_{dc}}{f_{sw} \times \Delta V_{dc}}$	D = 0.506 I_{dc} = 7.91 A V_{dc} = 48 V ΔV_{dc} = 10% of V_{dc} f_{sw} = 20 kHz	41.69 μ F
L_1	$\frac{D \times I_{dc}}{8 \times f_{sw}^2 \times C_f \times \Delta I_{L1}}$	D = 0.506 I_{dc} = 7.91 A f_{sw} = 20 kHz I_{L1} = 8.11 A ΔI_{L1} = 5% of I_{L1} C_f = 41.69 μ F	73.98 μ H
L_2	$\frac{D \times V_{mp}}{f_{sw} \times \Delta I_{L2}}$	D = 0.506 V_{mp} = 46.8 V f_{sw} = 20 kHz I_{L2} = $I_{mp} - I_{dc}$ ΔI_{L2} = 5% of I_{L2}	5.85 μ H
C_{dc}	$\omega_h = \frac{2 \times \pi \times f}{2 \times \pi \times N_r \times P} = \frac{120}{2 \times \pi \times N \times P}$ $\omega_l = \frac{2 \times \pi \times f}{2 \times \pi \times N \times P} = \frac{120}{2 \times \pi \times N \times P}$ $C_h = \frac{I_{dc}}{6 \times \omega_h \times \Delta V_{dc}}$ $C_l = \frac{I_{dc}}{6 \times \omega_l \times \Delta V_{dc}}$	P=6 N_r =3000 rpm N =800 rpm I_{dc} = 7.91 A V_{dc} = 48 V ΔV_{dc} = 10% of V_{dc}	C_h = 306.88 μ F C_l = 1092.8 μ F C_{dc} = 1000 μ F

TABLE 1

However, the language terms of fuzzy logics provide a practical way to define the functional characteristics of such a system. Fuzzy logic controllers are one symbolic controller. The proposed PV converters for DC-DC and DC-AC in this study comprise a power switch (S) controlled by a fuzzy-PID controller. To achieve high voltage gain, the proposed system creates a fuzzy-PID control for a brushless DC motor-based photovoltaic system, together with a three-level converter. The recommended control nevertheless yields the desired reference value even if the set points change. This control approach makes use of PID controllers as well as fuzzy logic. A PID controller frequently has parameter values that are proportional, integral, and derivative. With this controller architecture, oscillations can be reduced and the system's steady state inaccuracy can be controlled. When the load and set point are dynamic,

the recommended Fuzzy-PID controller is used to optimise and produce switching signals for the converter power switch. Fuzzy logics are utilised in this system to select the parameters Kp, Ki, and Kd. Three Kp, Ki, and Kd outputs as well as two inputs with delta k error and error comprise the input of the proposed fuzzy-PID controller. decreased use of the fuzzy-PID controller and settling time. The voltage source inverter's input source is increased by the designed Fuzzy-PID controller. The suggested Fuzzy-PID controller architecture block diagram for the dc landsman converter is shown in Figure 4.

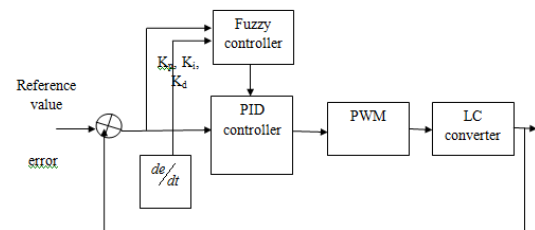


Fig 4 Fuzzy-PID controller Block Diagram

The two most important aspects of designing any fuzzy system are: 1. fuzzy rules; and 2. the selection and modification of membership functions.

Three scalar factors are selected in:

A new technique for improving the voltage, frequency, and current regulation of variable speed drives is developed using fuzzy logic mathematics. It may be utilised in EV applications to address problems that make non-linearity and its dynamic nature challenging to handle using conventional control techniques. This control has all the characteristics of this kind of problem.

As shown in Fig. 5, the fuzzy logic membership functions are categorised into five groups: five MF

for inputs and five MF for fuzzy sets of outputs. A Mamdani fuzzy inference system is used in this system to establish a connection between two input variables and one output variable. The two input variables are the error (e), which is the difference between the intended (set-point) and measured value, and the change of error (d), which deformalizes the specific variables of a conventional control gain.

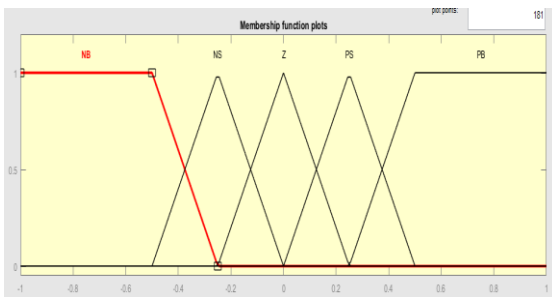


Fig 5 Membership function of FLC

Δwe	NB		NS		Z		PS		PB	
NB	NB	NB	NS	NS	NS	NS	NS	NS	Z	Z
NS	NB	NS	NS	NS	NS	Z	Z	PS	PS	PS
Z	NS	NS	NS	Z	Z	PS	PS	PS	PS	PS
PS	NS	Z	PS	PS	PS	PS	PS	PB	PB	PB
PB	Z	PS	PS	PS	PB	PB	PB	PB	PB	PB

Table II Fuzzy Rules

NB, NS, Z, PS, and PB, instead of just meaning negative big, negative small, zero, positive small, and positive large, respectively, can be used to generate a more precise continuous control rule by using the fundamental table of rules' interpolation. This instance selects symmetrical triangles with equal bases and a 50% overlap with adjoining MFs, excluding two hazy groups at the outer edges (which are selected as trapezoidal MFs). The system performance may be enhanced for EV applications by utilising this fuzzy controller in the outer loop and building the necessary control terms utilising the error signal and variation of error as input signals.

VI. SIMULATION IMPLEMENTAION

Simulink model for fuzzy-PID with LC converter; BLDC motor powered by photovoltaic array that is renewable. To control the high DC link voltage, low PV module energy is provided to the landsman converter. Three phase voltages are produced for BLDC motor running by feeding the DC voltage from the PV fed converter output to the VSI. In this recommended system, the primary Fuzzy-PID controller has offered to manage the response of the DC link voltage of the LC converter and reduce the settling time.

Figure 6 shows how the recommended controller, which regulates the converter's response, displays the Simulink model. The MPPT is used to produce the most power achievable.

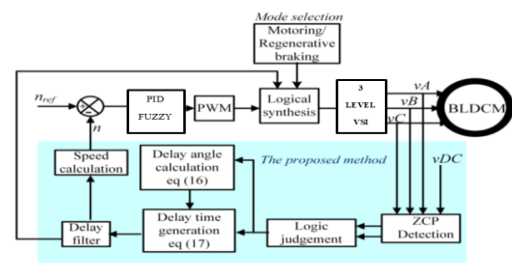


Fig6: Proposed Simulink Diagram

The switching signals are generated by the HC based on the valuation of the hall signal from the intended drive rotor angle. The sensor-less based back EMF method is used to calculate the voltage and current of the brushless DC motor stator. This estimate may be used to control the torque and speed of the proposed system. Using the proposed method, the location and speed of the rotor are accurately observed. The recommended cascaded multilevel inverter generates switching signals at the levels required to lower

harmonics in the carrier arrangement using a Pid based control method. A three-level inverter was used to produce the suggested system. The proposed circuit's Simulink implementation is shown in Figure 7, and Tables 3 and 4 provide illustrations of the system's parameters.

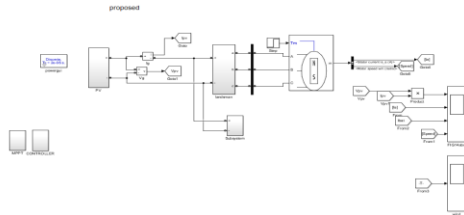


Fig7: Simulink Implementation of Proposed Circuit

Component of drive	Value
BLDC motor	48 V, 850 W (nominal), single speed, 7:1 gear arrangement
Solar-PV array	250 W (maximum)
Battery pack	Lithium-ion, 48 V, 100 Ah
Power converters	A 2-kW modified Landsman converter and A10 kW three-phase VSI

TABLE 3: SYSTEM PARAMETERS

BLDC motor parameter	Value
Stator per phase resistance, (R_{ph})	0.18 Ω
Stator per phase inductance, (L)	50 mH
Motor constant ($V_{peak}L \cdot L / k_{rpm}$)	33.513
Motor torque constant (Nm/Apeak)	0.32
Pole pairs	2
Inertia (kg.m ²)	0.02

Table 4: BLDC MOTOR SPECIFICATIONS

VII. SIMULATION RESULTS

A PMBLDC motor rated at 850 W will be used to thoroughly evaluate the proposed drive architecture.

Under different loading conditions and speeds, position sensor less control is employed. The following is a collection of the experimental results and relevant discussions.

1. Results of Solar PV System with MPPT Control

The input power to the drive is gradually changed in response to the available solar irradiation. An AC-DC converter enables the solar panel, battery, and wind to all supply power to the motor at the same time. Figure 8 shows that to maintain a consistent motor speed, battery power must rise as solar irradiation decreases. In the same way that battery power usage drops on a sunny day due to available solar irradiation. The speed of both transient scenarios is the same. A load torque of 1.4 Nm is applied during the process. a comparison between the fast load shift and converter output power. A redesigned Landsman converter, with shorter ripple and faster settling times, offers better stability.

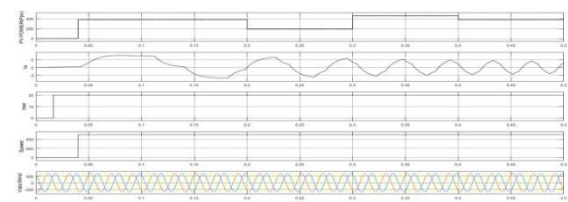


Fig8: Pv Power, Stator Current, Battery Current Motor Speed, Wind Voltage

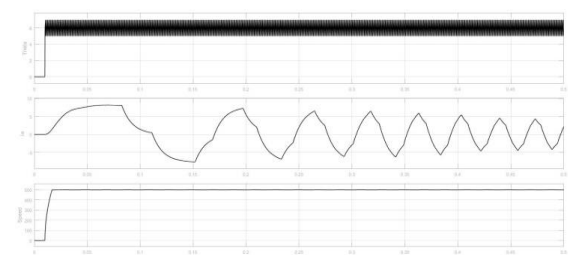


Fig9: Theta, IA, Speed

2. BLDC MOTOR DRIVE PERFORMANCE WITH POSITION SENSORLESS

The proposed system's theta and stator currents, as well as its speed, are shown in Fig. 9 under steady state conditions. The sensor less algorithm takes over as soon as the rotor accelerates. Initially, two phases are activated using predefined commutation logic to align the rotor to a predefined location. Phase current is nearly twice as high as the rated current to supply the high beginning torque required by the EV. Unlike the 400 ms forced acceleration time required by the LPF-based nonsensical control, our proposed method switches to the Sensor less running mode in roughly 230 ms. The load torque is initially adjusted to 3 Nm. The current regulation limits any surge during start-up, enabling a smooth and rapid startup.

3. AT DIFFERENT SPEED CONDITIONS

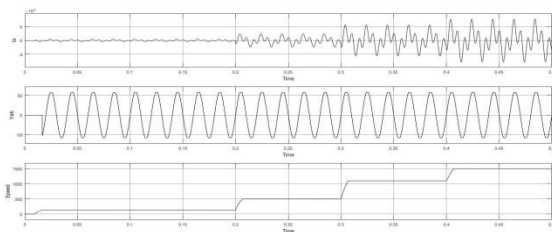


Fig10. Performance OF System under Different Speed Conditions at 130 rpm, 500 rpm, 1100 rpm

Fig. 10 illustrates the effect of the proposed commutation error correcting logic on the phase current at different speeds. The suggested approach is compared to the traditional LPF-based delay compensation logic for this EV application, and a noticeable reduction in current ripple is observed. At high speeds, the current ripple utilising the technique gets worse. This is the result of the flawed ZCPs. The current spike that occurs during commutation is

caused by the unbalanced dc link voltage and the software's calculation delay, even if the LPF-based approach also takes this into consideration. The suggested method maintains the shape of the current profile and controls the current ripple. Consequently, the proposed compensation strategy makes the sensor less commutation possible by removing current spikes.

4. PERFORMANCE UNDER DIFFERENT LOAD CONDITIONS:

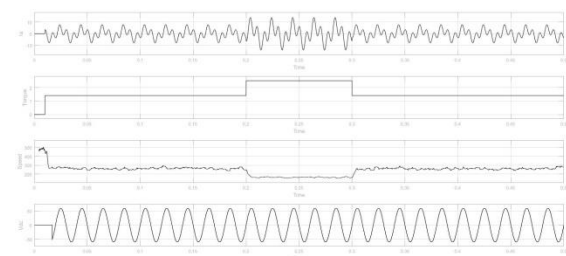


Fig11: Ia, Torque, Speed, Vab

The dynamic performance of the drive as the load changes is shown in Fig. 11. It is evident when the load reaches the rated 2.6 Nm since there is a small decrease in speed and an increase in current. When the load is reduced to half of the rated torque, the current drops. In both cases, the dc bus voltages are stable, suggesting that the speed is stable in stable equilibrium. However, there are momentary, minute overshoots and undershoots in speed during transient.

CONCLUSION:

Through modelling and application to the developed system, the study investigated the initial, dynamic, and steady-state characteristics of a proposed solar PV array-based BLDC motor-driven E-rickshaw with a Landsman converter. In addition to eliminating the need for external filters, a Landsman converter significantly lessens module current oscillations caused by snubber components. The PV-wind hybrid system Through modelling and application to the developed system, the study investigated the initial, dynamic, and steady-state characteristics of a proposed solar PV array-based BLDC motor-driven E-rickshaw with a Landsman converter. External filters can be avoided by utilising a Landsman converter, which also lessens oscillations in the module current that arise from snubber components. The commutation points are calculated by this position Sensor less control using the voltage level and the dc bus voltage. Significant current ripple, a distorted current profile, and incorrect commutation are the outcomes of any imbalance or fluctuation in the bus voltage. By significantly lowering current ripples, the proposed method produces a dependable and seamless Sensor less commutation. By employing freewheeling signals to estimate the commutation time, this strategy reduces interference pulses. With the updated Landsman converter, MPPT performance has increased dramatically. Furthermore, the regenerative braking makes the system incredibly energy-efficient. As a result, the recommended strategy is workable and appropriate for BLDC vehicle applications for inexpensive light-electric vehicles.